Chemical Science

Accepted Manuscript

This article can be cited before page numbers have been issued, to do this please use: X. Xiao, L. Tao, M. Li, X. Lv, D. Huang, X. Jiang, H. Pan, M. Wang and Y. Shen, *Chem. Sci.*, 2018, DOI: 10.1039/C7SC04849A.

ROYAL SOCIETY OF CHEMISTRY

rsc.li/chemical-science

View Article Online
DOI: 10.1039/C7SC04849A

Chemical Science

PAPER

Electronic Modulation of Transition Metal Phosphide via Doping as Efficient and pH-universal Electrocatalysts for Hydrogen Evolution Reaction

Received 00th January 2017,
Accepted 00th January 2017

DOI: 10.1039/x0xx00000x

www.rsc.org/

Xin Xiao,[a] Leiming Tao,[a] Man Li,[a] Xiaowei Lv,[a] Dekang Huang,[b] Xingxing Jiang,[a] Haiping Pan,[a] Mingkui Wang,[a] Yan Shen*[a]

It is highly desirable to develop efficient and low-cost catalysts to minimize the overpotential of hydrogen evolution reaction (HER) for large-scale hydrogen production from electrochemical water splitting. Doping foreign element into the host catalysts has been proposed as an effective approach to optimize the electronic characteristics of catalysts and thus improve their electrocatalytic performance. Herein we for the first time report vanadium doped CoP on self-supported conductive carbon cloth (V-CoP/CC) as a robust HER electrocatalyst, which achieves ultra-low overpotentials of 71, 123 and 47 mV to afford a current density of 10 mA cm^{-2} in 1 M KOH, 1 M PBS and 0.5 M H_2SO_4 media, respectively. Meanwhile, the V-CoP/CC electrode exhibits small Tafel slope and superior long-term stability over a wide pH range. Detail characterizations reveal that the modulation of electronic structure contributes to the superior HER performance of V-CoP/CC. We believe that the doping engineering opens up new opportunities to improve the HER catalytic activity of transition metal phosphides through regulating their physiochemical and electrochemical properties.

Introduction

The growing concerns on severe environmental pollution and rapid fossil fuel depletion have stimulated global effort to develop renewable and sustainable energy sources. Hydrogen as energy carrier provides a promising alternative to the traditional fossil fuel due to its high energy density and zero emission of greenhouse gas.[1-3] It is commonly acknowledged that generation of hydrogen from water splitting is more environmentally friendly than through the ways of steam methane reforming or coal gasification. However, the sluggish kinetics of the cathodic hydrogen evolution reaction (HER) and anodic oxygen evolution reaction (OER) in overall water splitting often require efficient electrocatalysts to reduce the electrolytic overpotential.[4] Up to date, noble metal Pt-based materials are considered to be the state-of-the-art catalysts for the HER. However, noble metal catalysts often suffer from high cost and limited abundance, which inevitably hinders its feasibility in large-scale production.[5,6] Furthermore, the water-splitting devices based on proton exchange membrane (PEM) technology and microbial electrolysis cells (MEC) often operate in acidic and neutral media, respectively. Besides, the water electrolysis in industry are usually performed in strongly basic media.[7-9] Therefore, exploring high-active, cost-effective, and earth-abundant HER catalysts that can operate well over a wide pH range would be highly desirable for practical applications.

At present, transition metal-based catalysts such as chalcogenides,[10,11] phosphides,[12,13] carbides/nitrides,[14,15] and alloys[16,17] have received considerable attention due to their outstanding electrocatalytic performance. Among these materials, binary Co-based phosphides formed by alloying of cobalt and phosphorus exhibit efficient activity for hydrodesulfurization (HDS), and thus come into attention for HER more recently due to the commonalities among catalysts for HDS and HER. Besides, the negatively charged phosphorus atoms in Co-based phosphides can efficiently capture protons due to the existence of strong electrostatic affinity while the positively charged cobalt atoms can function as hydride-acceptor sites. These properties synergistically promote the HER activity.[18,19] Furthermore, transition metal phosphides exhibit high stability for HER over a wide pH range. Above mentioned characteristics place them in the ranks of excellent nonprecious catalyst for HER. More recently, ternary transition metal phosphides have received more attention because their electrocatalytic performance outperforms that of the corresponding binary metal phosphides, which is mainly attributed to the modulation of the electronic structure in the multimetal phosphides.[20-22] Similarly, doping a foreign element into the host material could induce the change in the charge states through the occupation and energy of the anti-bonding defect levels, and thus it would be another efficient method to realize highly active catalysts for HER.[23,24] Besides,

[a] Wuhan National Laboratory for Optoelectronics, Huazhong University of Science and Technology, Wuhan 430074, P. R. China. *E-mail: mingkui.wang@mail.hust.edu.cn & cica_sheny@mail.hust.edu.cn
[b] College of Science, Huazhong Agricultural University, Wuhan 430070, P. R. China
Electronic Supplementary Information (ESI) available: Additional SEM, XRD and CV curves analysis. See DOI: 10.1039/x0xx00000x

View Article Online
DOI: 10.1039/C7SC04849A

vanadium, a cheaper and earth-abundant transition metal element, has attracted considerable attention for application in electrocatalytic field very recently. For instance, Sun's group have successfully incorporated vanadium element into $Ni(OH)_2$ and the formed NiV-LDH catalyst even precedes the best-performing non-precious NiFe-LDH material in catalyzing water oxidation.[25] The superior catalytic activity for NiV-LDH is attributed to the enhanced conductivity, facile electron transfer, and abundant active sites, indicating the metal vanadium would be an excellent foreign dopants.

Inspired by above discussion, we herein propose a scheme to develop an active catalyst for HER through incorporating transition metal vanadium into two-dimensional (2D) nanoneedle arrays of cobalt phosphide. The highly active and stable electrocatalyst can be scalable synthesized *via* hydrothermal-phosphorization method. Meanwhile, the three-dimensional (3D) conductive and flexible carbon cloth (CC) with high surface area was selected as substrates for supporting the catalytic material. As a resultant material, the V-CoP/CC electrode requires ultra-low overpotentials of 71, 123 and 47 mV to afford a current density of 10 mA cm^{-2} in 1 M KOH, 1 M PBS and 0.5 M H_2SO_4 media, respectively. Meanwhile, the V-CoP/CC electrode exhibits small Tafel slope and superior long-term stability over a wide pH range. Detailed investigation reveals that incorporation of vanadium component into CoP modulates the electronic structure of Co electrocatalytically active center and thus further boosts the intrinsic activity of CoP.

Experiments

Materials:

Nickel nitrate hexahydrate ($Co(NO_3)_2{\cdot}6H_2O$), vanadium chloride (VCl_3), urea ($CO(NH_2)_2$), ammonium fluoride (NH_4F), sodium hypophosphite monohydrate ($NaH_2PO_2{\cdot}H_2O$), potassium hydroxide (KOH), sulfuric acid (H_2SO_4), disodium hydrogen phosphate (Na_2HPO_4), sodium dihydrogen phosphate dihydrate ($NaH_2PO_4{\cdot}2H_2O$), acetone, and ethanol were all purchased from Beijing Chemical Co. Ltd (China). The commercial Pt/C (20 wt %) catalyst and Nafion solution (5 wt %) were purchased from Johnson Matthey and Sigma-Aldrich, respectively. All chemicals were used as-received. The deionized water (18.2 MΩ cm) was used throughout all the experiments.

Preparation of CoP/CC and V-CoP/CC

The substrate CC (2.5 × 4 cm^2) was cleaned sequentially in acetone, ethanol, and water solution for 15 min through sonication treatment. The preparation of V-CoP/CC nanoneedle arrays on the CC was similar to the reported work.[26] In a typical synthesis, 2.7 mmol of $Co(NO_3)_2{\cdot}6H_2O$, 0.3 mmol of VCl_3, 15 mmol of $CO(NH_2)_2$, and 9 mmol of NH_4F were dissolved in 80 mL of deionized water under vigorous stirring. Afterwards, the cleaned CC was immersed into the solution and transferred into the Teflon-lined stainless steel autoclave, and then reacted at 120 °C for 6 hrs in an electric oven. After the autoclave was cooled to room temperature, the CC with active materials was taken out and washed by water and ethanol, and finally dried at 60 °C overnight to obtain V-Co(OH)F/CC precursor. To further prepare V-CoP/CC, the precursor V-Co(OH)F/CC and NaH_2PO_2 were put in tube furnace, and then annealed at 350 °C for 120 min at a heating rate of 2 °C min^{-1} in N_2 atmosphere. The $V_xCo_{1-x}P$/CC (x represents the molar ratio of V and Co in the as-prepared materials, x=0.05, 0.15) materials were also prepared with the same method. Meanwhile, the preparation process of CoP/CC was similar to V-CoP/CC except without addition of VCl_3.

Material characterization

All X-ray diffraction (XRD) tests were conducted on X'pert PRO diffractometer (PANalytical B.V.) to characterize the crystal phases of the as-prepared materials. Meanwhile, the morphology and chemical elements composition of the catalyst were characterized by scanning electron microscope (SEM) and energy dispersive X-ray spectrometry (EDX), respectively, which were performed on Nova NanoSEM 450 (FEI Company). The lattice fringes of the as-obtained materials were performed on the transmission electron microscope (TEM) using Tecnai G2 F30 microscope. To further analyze the chemical binding states of various ions in the material, the X-ray photoelectron spectroscopy (XPS) characterizations were employed on a VG Multilab 2000. Gas chromatography (GC) analysis was performed on GC-2020 to investigate the faradic efficiency.

Electrochemical measurements

All the electrochemical tests were performed in three-electrode electrochemical cell using the CHI 660D electrochemical workstation. The carbon rod and as-prepared catalysts were used as the auxiliary electrode and the working electrode, respectively. Saturated calomel electrode (SCE) and Hg/HgO electrode were used as the reference electrodes in acid solution and alkaline solution, respectively. For a better comparisons, the state-of-the-art Pt/C electrode was also prepared *via* depositing commercial Pt/C on the CC substrate. All presented potentials in our work were converted to a commonly used reversible hydrogen electrode (RHE). The conversion formula are $E_{RHE} = E_{SCE} + 0.242 + 0.0594 \times pH$ and $E_{RHE} = E_{Hg/HgO} + 0.098 + 0.0594 \times pH$ for SCE and Hg/HgO reference electrodes, respectively. All the polarization curves were recorded with 95% *iR* compensation.

Results and discussion

Figure 1 depicts the design and integration of V-CoP

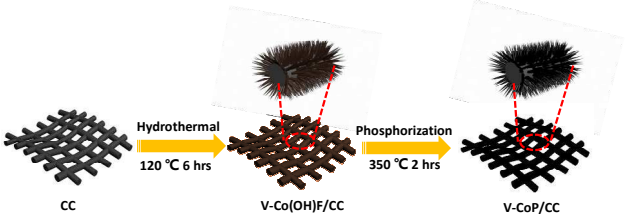

Figure 1. Schematic representation of V-CoP/CC preparation.

View Article Online
DOI: 10.1039/C7SC04849A
Chemical Science PAPER

nanoneedle arrays on CC to realize high activity and cost-effective catalyst for HER. In brief, the precursor V-Co(OH)F/CC nanoneedle arrays were firstly grown on CC *via* hydrothermal method, followed by phosphatizing the precursor V-Co(OH)F/CC using NaH_2PO_2 as phosphorus source to obtain V-CoP/CC. The precursor changed from pink to light brown after the vanadium doping (Figure S1). Besides, the CoP/CC and V-CoP/CC both show dark black after the process of phosphatizing. Meanwhile, scanning electron microscope (SEM) characterization shows that the nanoneedle-like arrays Co(OH)F and V-Co(OH)F (Figure S2a and S2b) are uniformly grown on CC substrates and the surface morphology shows no obvious change after a phosphorization process to form CoP and V-CoP/CC (Figure 2a and 2b). However, the size of the V-CoP/CC is slightly larger than the pure CoP, clearly implying that the introduction of V could effectively modulate the morphology of CoP. The transmission electron microscope (TEM) image (Figure 2c) further verified the nanoneedle-like structure of V-CoP. The lattice fringes with distance of 0.247 nm and 0.279 nm shown in high-resolution transmission electron microscope (HRTEM) images (Figure 2d) correspond well with the d-spacing of (111) and (002) planes of CoP, respectively.[27,28] It should be noted that there no any lattice fringe were observed for V-based phosiphides. However, the elemental mapping (Figure S3a-3d) confirmed the existence of V element in the V-CoP/CC. Above results indicate that the V may not exist in the form of crystalline compounds, and more characterizations will be presented in the following discussion to verify this opinion. The appearance of O element can be attributed to the surface oxidation during exposure in air.[29]

X-ray diffraction (XRD) analysis was further applied to investigate the crystalline phase and composition of as-prepared materials. As shown in Figure S4a and Figure 3a, all the diffraction peaks for the precursor V-Co(OH)F and the corresponding phosphide V-CoP are indexed to Co(OH)F

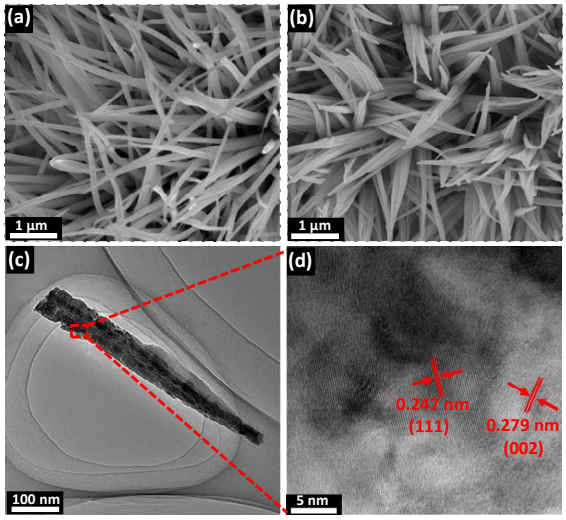

Figure 2. (a) and (b) SEM images of CoP/CC and V-CoP/CC, respectively. (c) and (d) HRTEM images of V-CoP/CC at different magnifications.

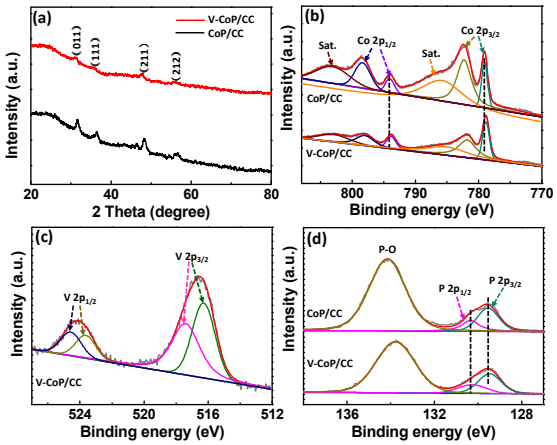

Figure 3. (a) XRD patterns of V-Co(OH)F/CC and V-CoP/CC. XPS spectra in the (b) Co 2p, (c) V 2p, and (d) P 2p regions for V-CoP/CC and CoP/CC.

(JCPDS 50-0827) and CoP (JCPDS 29-0497), respectively,[26] indicating the addition of vanadium does not induce the formation of V-based compounds in our case. The intensities of diffraction peaks in V doping system are lower than that for pure CoP, which could be probably caused by their low crystallinity. Besides, the diffraction peak at about 32° for V-CoP/CC shifts to smaller angle compared with that for pure CoP (Figure S4b), indicating the V doped CoP has a larger lattice constant than the pure CoP and indeed verify that V has been doped into the crystal lattice of CoP. Raman spectroscopy characterization was performed on the $V_xCo_{1-X}P$/CC (x=0, 0.05, 0.1, 0.15) to further investigate the surface chemical species. As shown in Figure S5, all the characteristic Raman peaks for $V_xCo_{1-X}P$/CC (x=0.05, 0.1, 0.15) are similar to the pure CoP. This result further confirms the formation of V doped compounds. Additionally, the introduction of vanadium probably induces Co atoms with lower positive charge in CoP due to the metallic nature of vanadium. Hence, we accordingly studied the composition evolution of CoP and V-CoP with X-ray photoelectron spectroscopy (XPS) analysis. As shown in Figure 3b, the binding energies (BEs) at 778.8 and 793.9 eV are assigned to the Co with partial positive charge for CoP in V-CoP/CC.[30,31] The XPS spectrum for V 2p in V-CoP exhibits two pairs of peaks, which are assigned to the surface oxidized V species such as V^{4+} (located at 516.2 and 523.7 eV) and V^{5+} (located at 517.3 and 524.8 eV) due to exposure in air (Figure 3c).[32] The peaks at BEs of 129.5 and 130.3 eV for P 2p in V-CoP are assigned to P with partial negative charge in the phosphide and at BE of 133.8 eV corresponds to the phosphate due to surface oxidation (Figure 3d).[31] Meanwhile, the high-resolution Co 2p and P 2p spectra for pure CoP were used as a control to explore the effect of vanadium doping on the electronic structure of CoP (Figure 3b and 3d). Obviously, the peaks for Co and P in V-CoP shift toward lower BEs compared with the ones in CoP, indicating an increase of electronic density in CoP after incorporation of V element. This implies a strong electron interaction between Co and V in V-

View Article Online
DOI: 10.1039/C7SC04849A

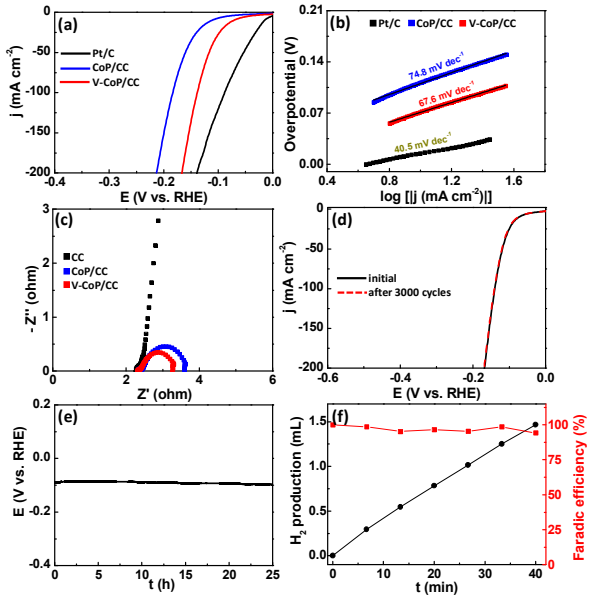

Figure 4. (a) HER polarization curves of bare Pt/C, CoP/CC, and V-CoP/CC in 1 M KOH. (b) the corresponding Tafel of the catalysts in 1 M KOH. (c) Nyquist plots of bare CC, CoP/CC and V–CoP/CC from 10 kHz to 0.01 Hz at −0.2 V vs. RHE. (d) Polarization curves of V-CoP/CC at the first cycle and after 3000 cycles. (e) The chronopotentiometric curve with a constant current density of 10 mA cm^{-2} for 25 h in 1 M KOH. (f) Faradic effciency (right *y* axis) and H_2 production (left *y* axis) over a period of 40 mins electrolysis at the current density of about 5 mA cm^{-2}.

CoP system. In short, above XRD, HRTEM, and XPS analysis results all demonstrate that there is no other form of crystalline V-based phosphides in the product. This implies that the as-prepared catalyst is vanadium doped CoP compound rather than a mixture of CoP and V-based phosphides. Meanwhile, the vanadium doping exhibits a strong influence on the electronic of the host catalyst CoP.

Considering that the strong electron interaction induced by vanadium incorporation could alter the HER kinetics on CoP, we thus evaluated the HER catalytic activity of the as-prepared samples by recording polarization curves in 1 M KOH solution. As shown in Figure S6, $V_{0.1}Co_{0.9}P$/CC shows the lowest overpotential among $V_xCo_{1-x}P$/CC catalysts (x=0, 0.05, 0.1, 0.15) to afford a current density of 10 mA cm^{-2}. In view of the $V_{0.1}Co_{0.9}P$/CC displays the optimal catalytic performance for HER, we thus set it as the focus in the following discussion and abbreviate it as V-CoP/CC. Besides, the mass loading of the active material $V_{0.1}Co_{0.9}P$ on CC substrate is 3.18 mg cm^{-2}. The actual doping molar concentration of V in $V_{0.1}Co_{0.9}P$/CC is about 5.9% obtained by inductively coupled plasma mass spectrometry (ICP-MS) analysis (Table S1). As shown in Figure 4a, the overpotential required for V-CoP/CC is 71 mV to generate a current density of 10 mA cm^{-2}, which is significantly lower than that for CoP/CC (112 mV). Moreover, the current density at overpotential of 150 mV for V-CoP/CC electrode is 137 mA cm^{-2}, being about 4 times higher than that for pure CoP/CC electrode. This demonstrates a remarkably enhanced HER activity *via* the vanadium doping in CoP. To further understand the HER mechanism, the Tafel plots were fitted with an equation of $\eta=b\log(j)+a$ (where η is the overpotential, *b* is the Tafel slope, and *j* is the current density).[33] As shown in Figure 4b, the obtained Tafel slopes of 67.6 and 74.8 mV dec^{-1} for V-CoP/CC and CoP/CC, respectively, lie within the range of 40 to 120 mV dec^{-1}. This means a Volmer-Heyrovsky mechanism for the HER on these electrodes surface where an adsorbed hydrogen atom electrochemically reacting with a proton to produce H_2 is the rate determining step on both electrodes. Besides, a relatively lower Tafel slope indicates a faster kinetics for V-CoP/CC, and thus a higher hydrogen generation rate was achieved on V-CoP/CC electrode compared with CoP/CC electrode. Moreover, the obtained exchange current density (j_0) based on the intercept of the Tafel plot for V-CoP/CC was as high as 0.897 mA cm^{-2}, which is about 2.7 times higher than that for CoP/CC (0.336 mA cm^{-2}), indicating a faster HER kinetics on V-CoP/CC electrode. The increased activity is probably attributed to the small charge transfer resistance.[34,35] This is further confirmed by electrochemical impedance spectroscopy (EIS) measurements, showing that indeed the V-CoP/CC electrode has a smaller polarization resistance than that of CoP/CC (Figure 4c). It suggests an enhanced charge transfer rate and faster catalytic kinetics on the V-CoP/CC electrode. Figure S7 shows a

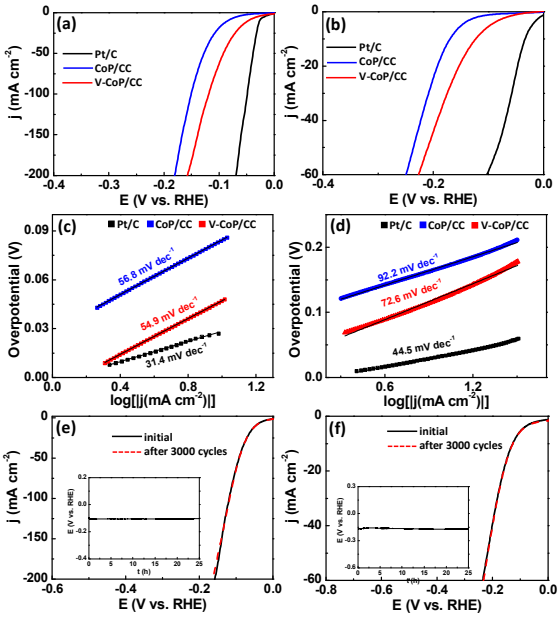

Figure 5. (a) and (b) HER polarization curves of bare Pt/C, CoP/CC, and V-CoP/CC in 0.5 M H_2SO_4 and 1 M PBS, respectively. (c) and (d) the corresponding Tafel of the catalysts in in 0.5 M H_2SO_4 and 1 M PBS, respectively. (e) and (f) Polarization curves of V-CoP/CC at the first cycle and after 3000 cycles in 0.5 M H_2SO_4 and 1 M PBS, respectively, and the insert is the chronopotentiometric curve with a constant current density of 10 mA cm^{-2} for 25 hrs in 0.5 M H_2SO_4 and 1 M PBS, respectively.

View Article Online
DOI: 10.1039/C7SC04849A

multistep current polarization curve for the V-CoP/CC electrode. The potential immediately levels off at about -0.09 V at the beginning and then remains no obvious change for the rest 1 h. The other steps also show similar behavior, implying the good mechanical robustness, conductivity and mass transportation of V-CoP/CC electrode.[36]

The stability is another key issue to evaluate the catalysts for practical application which is quite challenging for noble metal-free HER catalysts. To evaluate the catalyst stability in strong alkaline solution, we carried out linear scanning voltammetry (LSV) after repeated CV cycles between -0.2 and -0.1 V (vs. RHE). The LSV curves of V-CoP/CC before and after 3,000 cycles in 1 M KOH are shown in Figure 4d. The catalyst performs efficiently without notable loss of cathodic current density after 3,000 cycles. Furthermore, the V-CoP/CC exhibits a small fluctuation in potential at a fixed current density of 10 mA cm^{-2} after 25 hrs chronopotentiometric test (Figure 4e), indicating the excellent stability of the V-CoP/CC electrode in strong alkaline media. Besides, the V-CoP/CC electrode shows about 97% Faraday efficiency over a period of 40 mins electrolysis process at a current density of about 5 mA cm^{-2} in 1 M KOH (Figure 4f), indicating an efficient electrons transfer in the process of hydrogen generation from water splitting.

The prepared HER catalysts that can operate at a wide pH range will certainly be of great utility due to the inevitable proton concentration change during practical deployment. Therefore, we evaluated the HER catalytic activity of V-CoP/CC in 1 M phosphate-buffered saline (PBS, pH=7) and 0.5 M H_2SO_4 (pH=0) media. As shown in Figure 5a and 5b, the V-CoP/CC electrode needs overpotentials of only 123 and 47 mV to afford an current density of 10 mA cm^{-2} in 1 M PBS and 0.5 M H_2SO_4, respectively. The relatively high overpotential in 1 M PBS media is probably caused by the low ion migration in PBS solution and thus results in a lower intrinsic kinetics during the process of HER.[37] Meanwhile, the obtained Tafel slopes of 72.6 and 54.9 mV dec^{-1} for V-CoP/CC in 1 M PBS and 0.5 M H_2SO_4, respectively, are lower than those for the pure CoP/CC (Figure 5c and 5d). This implies a higher hydrogen generation rate was achieved on V-CoP/CC. As shown in Figure 5e and 5f, both polarization curves before and after 3,000 cycles test show no obvious change in 1 M PBS and 0.5 M H_2SO_4, respectively, as well as a small fluctuation in overpotentials were observed to afford the current density of 10 mA cm^{-2} in 1 M PBS and 0.5 M H_2SO_4 for 25 hrs stability test (insert in Figure 5e and 5f). All above discussion indicates that V-CoP/CC shows excellent catalytic activity and high stability for HER over a wide pH range, which provides a promising electrocatalyst for practical applications.

Conclusion

In summary, we have experimentally revealed that the electronic modulation of transition metal phosphide through foreign metal ions doping provides a new strategy to efficiently boost the HER activity. The as-obtained V-CoP/CC catalyst exhibits extremely low overpotential and superior long-term durability for HER over a wide pH range, which is a cost-effective alternative material for noble metal Pt-based HER electrocatalysts. The excellent electrochemical performance of V-CoP/CC is mainly attributed to strong electronic interaction. The material design present in this work broadens our vision to fabricate noble-metal free catalysts for other important reactions in electrochemical energy conversion and storage.

Conflicts of interest

There are no conflicts to declare.

Acknowledgements

This work was financially supported from the 973 Program of China (2014CB643506), the NSFC Major International (Regional) Joint Research Project NSFC-SNSF (51661135023), NSFC (21673091), the Fundamental Research Funds for the Central Universities (HUST: 2016YXMS031), the Director Fund of the WNLO, and the Open Funds of the State Key Laboratory of Electroanalytical Chemistry (SKLEAC201607). The authors thank the Analytical and Testing Center of HUST and the Center of Micro-Fabrication and Characterization of WNLO for the measurements.

Notes and references

1 A. J. Bard, M. A. Fox, *Acc. Chem. Res*., 1995, **28**, 141-145.
2 M. S. Dresselhaus, I. L. Thomas, *Nature*, 2001, **414**, 332-337.
3 S. D. Ebbesen, S. H. Jensen, A. Hauch, M. B. Mogensen, *Chem. Rev*., 2014, **114**, 10697-10734.
4 X. X. Zou, Y. Zhang, *Chem. Soc. Rev*., 2015, **44**, 5148-5180.
5 A. L. Goff, V. Artero, B. Jousselme, P. D. Tran, N. Guillet, R. Métayé, A. Fihri, S. Palacin, M. Fontecave, *Science*, 2009, **326**, 1384-1387.
6 R. Subbaraman, D. Tripkovic, D. Strmcnik, K. C. Chang, M. Uchimura, A. P. Paulikas, V. Stamenkovic, N. M. Markovic, *Science*, 2011, **334**, 1256-1260.
7 Z. H. Pu, Q. Liu, A. M. Asiri, Y. L. Luo, X. P. Sun, Y. Q. He, *Electrochim. Acta*, 2015, **168**, 133-138.
8 A. Kundu, J. N. Sahu, G. Redzwan, M. A. Hashim, *Int. J. Hydrog. Energy*, 2013, **38**, 1745-1757.
9 J. W. D. Ng, M. García-Melchor, P. Chakthranont, C. Kirk, A. Vojvodic, *Nat. Energy*, 2016, **1**, 16053.
10 Y. Yan, X. M. Ge, Z. L. Liu, J. Y. Wang, J. M. Lee, X. Wang, *Nanoscale*, 2013, **5**, 7768-7771.
11 L. Yu, B. Y. Xia, X. Wang, X. W. Lou, *Adv. Mater*., 2016, **28**, 92-97.
12 Q. Liu, J. Q. Tian, W. Cui, P. Jiang, N. Y. Cheng, A. M. Asiri, X. P. Sun, *Angew. Chem*., 2014, **126**, 6828-6832.
13 D. R. Liyanage, S. J. Danforth, Y. Liu, M. E. Bussell, S. L. Brock, *Chem. Mater*., 2015, **27**, 4349-4357.
14 X. D. Jia, Y. F. Zhao, G. B. Chen, L. Shang, R. Shi, X. F. Kang, G. I. N. Waterhouse, L. Z. Wu, C. H. Tung, T. R. Zhang, *Adv. Energy. Mater*., 2016, **6**, 1502585.
15 Y. Huang, Q. F. Gong, X. N. Song, K. Feng, K. Q. Nie, F. P. Zhao, Y. Y. Wang, M. Zeng, J. Zhong, Y. G. Li, *ACS Nano*, 2016, **10**, 11337-11343.
16 H. F. Lv, Z. Xi, Z. Z. Chen, S. J. Guo, Y. S. Yu, W. L. Zhu, Q. Li, X. Zhang, M. Pan, G. Lu, S. C. Mu, S. H. Sun, *J. Am. Chem. Soc*., 2015, **137**, 5859-5862.

View Article Online
DOI: 10.1039/C7SC04849A

17 Y. C. Hu, Y. Z. Wang, R. Su, C. R. Cao, F. Li, C. W. Sun, Y. Yang, P. F. Guan, D. W. Ding, Z. L. Wang, W. H. Wang, *Adv. Mater*., 2016, **28**, 10293-10297.
18 P. Liu, J. A. Rodriguez, *J. Am. Chem. Soc*., 2005, **127**, 14871-14878.
19 S. Anantharaj, S. Rao Ede, K. Sakthikumar, K. Karthick, S. Mishra, S. Kundu, *ACS Catal*., 2016, **6**, 8069-8097.
20 J. H. Hao, W. S. Yang, Z. Zhang, J. L. Tang, *Nanoscale*, 2015, **7**, 11055-11062.
21 T. T. Liu, X. Ma, D. N. Liu, S. Hao, G. Du, Y. J. Ma, A. M. Asiri, X. P. Sun, L. Chen, *ACS Catal*., 2016, **7**, 98-102.
22 H. F. Liang, A. N. Gandi, D. H. Anjum, X. B. Wang, U. Schwingenschlögl, H. N. Alshareef, *Nano Lett*., 2016, **16**, 7718-7725.
23 X. Q. Lin, J. Ni, *J. Appl. Phy*., 2016, **120**, 064305.
24 D. Y. Wang, M. Gong, H. L. Chou, C. J. Pan, H. A. Chen, Y. P. Wu, M. C. Lin, M. Y. Guan, J. Yang, C. W. Chen, Y. L. Wang, B. J. Hwang, C. C. Chen, H. J. Dai, *J. Am. Chem. Soc*., 2015, **137**, 1587-1592.
25 K. Fan, H. Chen, Y. F. Ji, H. Huang, P. M. Claesson, Q. Daniel, B. Philippe, H. Rensmo, F. S. Li, Y. Luo, L. C. Sun, *Nat. Commun*., 2016, **7**, 11981.
26 J. Q. Tian, Q. Liu, A. M. Asiri, X. P. Sun, *J. Am. Chem. Soc*., 2014, **136**, 7587-7590.
27 J. Y. Li, X. M. Zhou, Z. M. Xia, Z. Y. Zhang, J. Li, Y. Y. Ma, Y. Q. Qu, *J. Mater. Chem. A*, 2015, **3**, 13066-13071.
28 L. L. Li, X. Y. Lia, L. H. Ai, J. Jiang, *RSC Adv*., 2015, **5**, 90265-90271.
29 X. Xiao, D. K. Huang, Y. P. Luo, M. Li, M. K. Wang, Y. Shen, *RSC Adv*., 2016, **6**, 100437-100442.
30 C. Tang, R. Zhang, W. B. Lu, L. B. He, X. E. Jiang, A. M. Asiri, X. P. Sun, *Adv. Mater*., 2017, **29**, 1602441.
31 W. Gao, M. Yan, H. Y. Cheung, Z. M. Xia, X. M. Zhou,Y. B. Qin, C. Y. Wong, Y. Q. Qua, C. R. Chang, J. C. Ho, *Nano Energy*, 2017, **38**, 290-296.
32 K. Fan, Y. F. Ji, H. Y. Zou, J. F. Zhang, B. C. Zhu, H. Chen, Q. Daniel, Y. Luo, J. G. Yu, L. C. Sun, *Angew. Chem. Int. Ed*., 2017, **56**, 3289-3293.
33 G. T. Fu, Z. M. Cui, Y. F. Chen, Y. T. Li, Y. W. Tang, J. B. Goodenough, *Adv. Energy Mater*., 2017, **7**, 1601172.
34 F. Song, X. L. Hu, *Nat. Commun*., 2014, **5**, 4477.
35 L. Gao, D. K. Huang, Y. Shen, M. Wang, *J. Mater. Chem. A*, 2015, **3**, 23570-23576.
36 C. Tang, N. Y. Cheng, Z. H. Pu, W. Xing, X. P. Sun, *Angew. Chem. Int. Ed*., 2015, **54**, 9351-9355.
37 J. Wang, F. Xu, H. Y. Jin, Y. Q. Chen, Y. Wang, *Adv. Mater*. 2017, **29**, 1605838.

View Article Online
DOI: 10.1039/C7SC04849A

Table of contents entry

The electronic modulation of host catalyst via doping provides a new strategy to efficiently boost HER activity of transition metal phosphides.